RESEARCH ARTICLE OPEN ACCESS

Investigating the Presence of Neurodegeneration Independent of Relapses in MOGAD Compared to Relapsing-Remitting Multiple Sclerosis

Valentina Camera,[1,2] Silvia Messina,[1,*] Agnese Tamanti,[2,3,*] Pietro Bontempi,[3] Lorenzo Salvatore Petralia,[4] Ludovica Griffanti,[5,6] Marco Pitteri,[7,8] Maddalena Guandalini,[2] Francesca Benedetta Pizzini,[3] Gabriele C. DeLuca,[1] Maria Isabel S. Leite,[1] Alessandro Daducci,[9] Ruth Geraldes,[1] Massimiliano Calabrese,[2,†] and Jacqueline Palace[1,†]

Correspondence
Prof. Palace
jacqueline.palace@ndcn.ox.ac.uk

Neurol Open Access 2025;1:e000013. doi:10.1212/WN9.0000000000000013

Abstract

Background and Objectives

Neurodegeneration and progression independent of relapse activity (PIRA) are features of multiple sclerosis (MS), but their presence in myelin oligodendrocyte glycoprotein antibody–associated disease (MOGAD) is unclear. The aim of this study was to investigate neurodegeneration in MOGAD, independent of relapses, by comparing clinical, cognitive, and advanced MRI markers in MOGAD, relapsing-remitting MS (RRMS), and healthy control (HC).

Methods

In this prospective study, participants with MOGAD, those with RRMS, and HC participants from the Oxford National Service and the Verona MS Centre were recruited and monitored between January 2018 and January 2024. Inclusion criteria included no attacks in the previous 6 months and during the study period, with a minimum 12-month interval between baseline and follow-up assessments. Participants underwent clinical Expanded Disability Status Scale (EDSS) assessment, cognitive Brief Repeatable Battery of Neuropsychological Tests (BRBNTs), and 3T brain structural and diffusion MRI evaluations. Clinical and cognitive PIRA events were defined as relapse-independent increases in EDSS scores and declines in cognitive function (a decrease of at least 1 SD in at least two BRBNTs). Annual percentage changes in brain volume, total cortical/deep gray matter (DGM)/white matter volumes, and cortical thickness were derived from structural MRI. Neurite orientation dispersion and density imaging metrics were calculated in lesional and nonlesional white matter from diffusion MRI.

Results

Twenty patients with MOGAD; 32 with RRMS, matched for age, sex, baseline EDSS score, and cognitive impairment; and 21 HCs were recruited. Over a median follow-up of 17 months (range 12–45) for RRMS and 16 months (range 12–56) for MOGAD, clinical PIRA occurred in 6.25% of patients with RRMS and 0% of patients with MOGAD and cognitive PIRA in 6.67% of patients with RRMS and 0% of patients with MOGAD. Compared with HCs, patients with RRMS showed greater annualized thalamic ($\beta = -0.874$; 95% CI −1.384 to −0.364; $p = 0.001$), hippocampal ($\beta = -1.269$; 95% CI −2.230 to −0.308; $p = 0.010$), and DGM ($\beta = -0.920$; 95% CI −0.920 to −0.099; $p = 0.015$) atrophy while no significant changes occurred in patients with

MORE ONLINE

Supplementary Material

*These authors contributed equally to this work.

†These authors contributed equally to this work as co-senior authors.

[1]Nuffield Department of Clinical Neuroscience, University of Oxford, Oxford, OX39DU, United Kingdom; [2]Department of Neuroscience, Biomedicine and Movement Sciences, University of Verona; Verona, 37134, Italy; [3]Department of Engineering for Innovation Medicine (DIMI), University of Verona, Verona, 37134, Italy; [4]Department of Chemistry, Physical and Theoretical Chemistry Laboratory, University of Oxford, Oxford, OX13QZ, United Kingdom; [5]Department of Psychiatry, University of Oxford, Oxford, OX37JX, United Kingdom; [6]Oxford Centre for Human Brain Activity (OHBA), Wellcome Centre for Integrative Neuroimaging (WIN), University of Oxford; Oxford, OX37JX, United Kingdom; [7]Deapartment of Neuropsychology, National Hospital for Neurology and Neurosurgery, London, WC1N3BG, United Kingdom; [8]Department of Neuroinflammation, University College London, London WC1N1PK, United Kingdom; and [9]Department of Computer Science, University of Verona, Verona, 37134, Italy.

The Article Processing Charge was funded by the authors.

Glossary

BRBNTs = Brief Repeatable Battery of Neuropsychological Tests; **CDA** = confirmed disability accumulation; **DGM** = deep gray matter; **DGMV** = deep gray matter volume; **DIR** = double-inversion recovery; **dMRI** = diffusion-weighted imaging; **EDSS** = Expanded Disability Status Scale; **FMRIB** = Functional Magnetic Resonance Imaging of Brain; **FSL** = FMRIB Software Library; **HC** = healthy control; **ISOVF** = isotropic volume fraction; **MOGAD** = myelin oligodendrocyte glycoprotein antibody–associated disease; **MPRAGE** = magnetization-prepared rapid gradient echo; **MS** = multiple sclerosis; **NDI** = neurite density index; **NHS** = National Health System; **NLWM** = nonlesional white matter; **NODDI** = neurite orientation dispersion and density imaging; **NWM** = normal white matter; **ODI** = orientation dispersion index; **PBVC** = percentage of brain volume change; **PIRE** = progression independent of relapse activity; **RRMS** = relapsing-remitting MS; **sMRI** = structural MRI; **TBVC** = total brain volume change; **WM** = white matter; **WMV** = WM volume; **β** = β coefficient.

MOGAD. Patients with RRMS also had greater annualized thalamic (β = −0.742; 95% CI −1.330 to −0.083; $p = 0.011$) and hippocampal (β = −1.078; 95% CI −1.960 to −0.197; $p = 0.017$) atrophy compared with patients with MOGAD. Longitudinal increases in free water content within white matter lesions were observed in the RRMS group ($p = 0.008$) but not in the MOGAD group.

Discussion

The absence of PIRA and progressive brain damage independent of attacks distinguished MOGAD from RRMS. Further research with larger cohorts and longer follow-ups is needed to validate these findings.

Introduction

Progression independent of relapse activity (PIRA) is a novel clinical concept in multiple sclerosis (MS) that describes an insidious, persistent disability accrual not related to attacks,[1] occurring not only in progressive MS phenotypes but also in the early disease and relapsing-remitting phases (RRMS).[1,2] PIRA seems to reflect the presence of chronic smoldering inflammation and subsequent neurodegenerative pathobiological processes in MS.[2,3] Cognitive decline independent of relapse activity (cognitive PIRA) can be a sensitive measure of neurodegeneration in MS, even independent of clinical worsening,[4,5] and in other neurodegenerative conditions.[6,7] Longitudinal structural MRI (sMRI) brain volume loss, measured using MRI scans at different intervals, is a marker of progressive neuroaxonal loss and atrophy and has been used to assess treatment efficacy in MS.[8-11] White matter atrophy involves myelin and axonal loss, often caused by Wallerian degeneration. Gray matter atrophy is widespread, affecting areas such as the neocortex, thalamus, hippocampus, and cerebellum, and is mainly due to neuroaxonal loss and neuronal shrinkage rather than demyelination.[12-14]

Diffusion-weighted imaging (dMRI) is an advanced MRI approach allowing the evaluation of the microstructural brain tissue damage. Neurite orientation dispersion and density imaging (NODDI) is a water-diffusion model, which can interpret changes within one of the three compartments: intra-axonal (neurite density index—NDI), extraneurite (ODI), and free water (isotropic volume fraction—ISOVF).[15] The histopathologic validation studies on the NODDI model have shown significant correlations between the ODI and circular variance, a marker of neurite orientation variability, as well as between ODI and myelin staining fraction in MS samples.[16] Negative correlations were observed between the NDI and circular variance in healthy controls (HCs) and positive correlations between NDI and markers of myelin, axon, and microglia content.[16,17] These findings highlight NODDI's ability to explain neuroaxonal damage even in complex white matter regions, such as crossing fibers, which single-compartment models, such as diffusion tensor imaging, fail to depict accurately. Providing a more detailed understanding of tissue microstructure in MS, NODDI is considered a promising imaging marker to identify the disease progression and neurodegeneration.[3]

Despite diverse clinical findings revealing that PIRA is less common in myelin oligodendrocyte glycoprotein antibody–associated disease (MOGAD) compared with MS,[18,19] on the contrary, some other quantitative sMRI studies have suggested greater subclinical brain volume loss in MOGAD than in MS.[20,21] Nevertheless, prospective MRI studies comparing patients with MOGAD with healthy participants and patients with MS while controlling for interscan relapses, age, sex, and additional outcomes, including cognitive function and measures of microstructural tissue damage, are currently lacking. In agreement with the international panel of pediatric and adult neurologists, neuroimmunologists, and researchers experts in MOGAD, we hypothesize that clinical and cognitive progression, as well as neurodegenerative processes detected through imaging, independent of relapse activity, does not characterize MOGAD, in contrast to MS.[22] The aim of this study was to assess the presence of progression and neurodegeneration in MOGAD, independent of

relapses, in comparison with RRMS and HC. We primarily assessed the frequency of both clinical and cognitive PIRA events in a cohort of patients with MOGAD matched with an RRMS cohort. Second, we aimed to assess the presence of subclinical neurodegeneration by comparing longitudinal brain MRI volumetrics (total and regional) and NODDI MRI metrics across MOGAD, RRMS, and HC groups.

Methods

Study Cohort

Seventy-seven participants from the National Health System (NHS) England Commissioned Neuromyelitis Optica service in Oxford (United Kingdom) (MOGAD cohort n = 16, RRMS cohort n = 15, HC cohort n = 13) and the Verona Multiple Sclerosis Centre (Italy) (MOGAD cohort n = 6, RRMS cohort n = 18, HC cohort n = 9) were recruited and prospectively examined between January 2018 and January 2024. Inclusion criteria were as follows: (1) have clear positive myelin oligodendrocyte glycoprotein immunoglobulins G (MOG-IgG) on the live CBA and clinical features typical of adult-onset MOGAD (all fulfilled the recent MOGAD criteria[22]) or fulfilled the RRMS diagnostic criteria[23] or have HC status; (2) no attacks in the previous 6 months from baseline (T0) assessment; and (3) at least 12-month interval between the T0 and follow-up (T1) assessments. Exclusion criteria were as follows: (1) clinically confirmed attacks or therapy changes in between the T0 and T1 assessments; (2) concurrent disorders that may confound the data (e.g., dementia, cerebral small vessel diseases, and other systemic disabling autoimmune diseases). HCs were matched for age and sex at birth to the disease groups. A time lag of at least six months from the last attack to T0 assessment was chosen, consistent with similar published studies[24-26] and in consideration of lesion resolution dynamic in MOGAD.[27] At each study visit, patients underwent clinical Expanded Disability Status Scale (EDSS) assessment, cognitive Brief Repeatable Battery of Neuropsychological Tests (BRBNTs), and 3T brain advanced MRI assessments. HCs underwent 3T brain advanced MRI assessment at each study visit. After the T1 evaluation, patients attended a further EDSS evaluation at least 6 months from T1 (confirmation EDSS visit) (Figure 1).

Clinical and Cognitive PIRA Definitions

Demographic, clinical, and cognitive variables are provided in eTable 1. The EDSS assessment and BRBNTs were performed by experienced neurologists and neuropsychologists at each study visit. At the end of the follow-up, patients with confirmed disability accumulation (CDA), defined as an increase of EDSS score ≥1.5 if baseline EDSS score was 0, of EDSS score ≥1 if baseline EDSS score was 1–5, and of EDSS score 0.5 if baseline EDSS score was ≥5.5 (not related to worsening on cognitive section of the Kurtzke score), were identified.[1,9] Patients were classified having "clinical PIRA" if presenting CDA confirmed at a visit performed at least 6 months from T1 and no reports of recent relapses during the period between the EDSS increase to the confirmation of disability progression (confirmation EDSS visit).[1,9] We calculated z-scores for each BRBNT subtest considering available English[28] and Italian[29] HC cohorts. At T0, patients with scores below 1.5 SDs in at least two BRBNT subtests were classified as having cognitive impairment.[29,30] At the end of the follow-up, with the aim of capturing even minimal cognitive change over time, we adopted a stringent criterion by defining cognitive decline in those with a −1 SD decrease from the baseline z-score in at least two cognitive tests evaluating different cognitive domains. Patients were labeled with "cognitive PIRA" if presenting cognitive decline and no reports of relapses within 6 months from the cognitive decline event.

Brain MRI Acquisition and Processing

Brain MRI scans at T0 and T1 were acquired on a 3T Siemens MAGNETOM Prisma scanner fitted with a 64-channel head coil at the Oxford Centre for Functional Magnetic Resonance Imaging of Brain (FMRIB) and on a 3T Philips ELITION-S scanner fitted with a 32-channel head coil at the Verona University Hospital Neuroradiology Department. Oxford and Verona brain MRI acquisition protocols are provided in eTable 2.

Longitudinal sMRI Metrics of Volumetric Changes

Brain MRI data were pre-processed using FMRIB Software Library (FSL) 6.0.[31] Image pre-processing as well as cross-sectional and longitudinal quantitative volumetric MRI analyses were conducted as detailed in eAppendix 1. Among baseline imaging characteristics, cortical lesions number was calculated on 3D double inversion recovery (DIR) and 3D T1weighted/ Magnetization prepared rapid gradient echo imaging (MPRAGE) images by consensus between two raters (SM, MC) (eAppendix 1). SIENA[32] and Freesurfer longitudinal stream[33] were employed to obtain quantitative longitudinal MRI volumetrics from lesions-filled T1-weighted/3D MPRAGE images at baseline (T0) and follow-up (T1). Longitudinal analyses included quantification of new asymptomatic T2/FLAIR hyperintense lesions (new T2L number), annualised percentage brain volume change (PBVC/yr - SIENA), and annualised total brain volume change (TBVC/yr - Freesurfer). In addition, annualized longitudinal alterations in white matter volume (WMV/yr), deep gray matter volume (DGMV/yr), cortical volume (CtxV/yr), cortical thickness (CTh/yr), thalamus, caudate, putamen, pallidum, hippocampus, amygdala, and nucleus accumbens mean volumes were evaluated.

Longitudinal NODDI Metrics of Tissue Integrity Changes

dMRI scans were acquired in the Oxford cohort (MOGAD cohort n = 14, MS cohort n = 14, HC cohort n = 12), and after preprocessing, the NODDI model was fitted using the publicly available Accelerated Microstructure Imaging via Convex Optimization (AMICO) software program (eMethods 1) to obtain NDI, ISOVF, and ODI quantitative brain maps at T0 and T1 dMRI time points. The mean NODDI parameters were calculated within T2-FLAIR hyperintense white matter lesions (WM lesions) and nonlesional white matter (NLWM) masks of patients with RRMS and MOGAD and within

Figure 1 Study Design and Methods

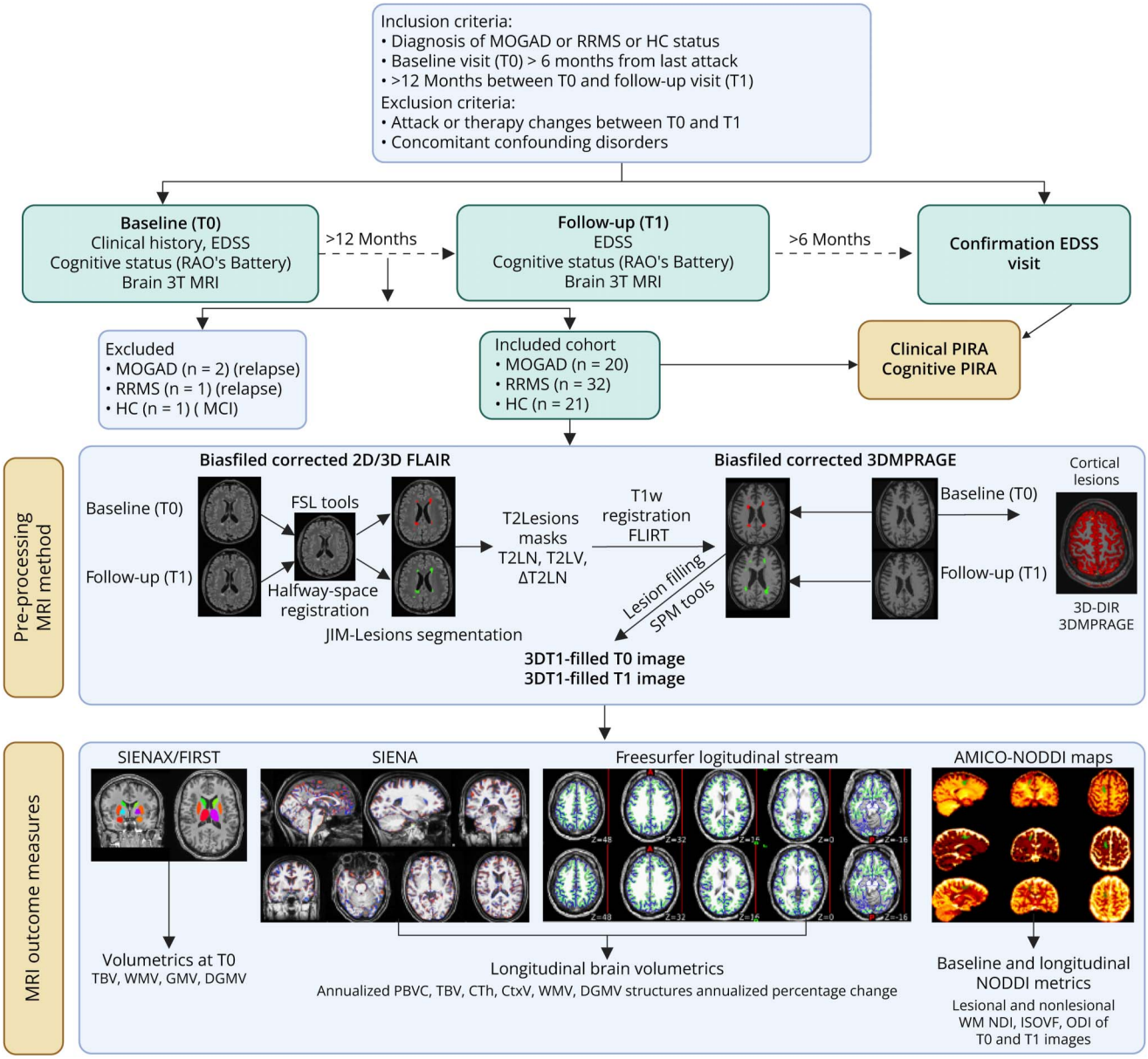

ΔT2LN = variation of T2LN between T0 and T1 MRI; ΔT2LV = variation of T2LV between T0 and T1 MRI; CLN = cortical lesion number at T0 MRI; Cth = cortical thickness; CtxV = cortical volume; DGMV = deep gray matter volume; EDSS = Expanded Disability Status Scale; GMV = gray matter volume; HC = healthy control; ISOVF = isotropic volume fraction; MOGAD = MOG antibody–associated disease; NAWM = normal-appearing white matter; NDI = neurite density index; NODDI = neurite orientation dispersion and density index; ODI = orientation dispersion index; PBVC = percentage of brain volume change; RRMS = relapsing-remitting MS; T2LN = T2/FLAIR hyperintense lesions number; T2LV = T2/FLAIR hyperintense lesion volume; TBV = total brain volume at T0; WM = white matter; WMV = white matter volume. Created with Biorender.com.

normal white matter (NWM) masks of HCs at T0 and T1 dMRI scans.

Overall methods deployed in this prospective study are illustrated in Figure 1.

Statistical Analysis

All the statistical analyses were performed using STATA14. Baseline continuous clinical and cognitive variables, as well as sMRI volumetrics or dMRI NODDI metrics, were compared across groups using the unpaired *t* test and the Kruskal-Wallis test while the χ^2 test was used to compare baseline categorical variables across MOGAD, RRMS, and HC groups.

Our aim was to investigate the presence of neurodegeneration independent of relapses in MOGAD compared with RRMS and HC, using surrogate clinical, cognitive, and neuroimaging markers of neurodegenerative processes independent of relapses.

We primarily verified the frequency of "clinical PIRA" and "cognitive PIRA" events in the MOGAD cohort compared with an RRMS cohort matched for age, sex, baseline clinical

and cognitive disability, and similar follow-up durations, and we compared these frequencies using the Fisher exact test.

We then analyzed subclinical sMRI and MRI metrics of neurodegeneration comparing MOGAD vs HC, RRMS vs HC, and MOGAD vs RRMS. Longitudinal brain MRI volumetrics were analyzed using linear mixed-effect models exploring the associations between the longitudinal annualized brain MRI volumetrics (dependent variables) and the disease cohorts (explanatory variable). The model incorporated age, sex, time from last relapse at T0, and new T2Ls at T1 as explanatory covariates, with the MRI protocol (one for each of the two centers) as the random intercept. β coefficients (β), representing the average effects of the explanatory variables on the dependent variable (fixed effects), are provided. Longitudinal NODDI metrics within lesional and nonlesional WM masks between T0 and T1 dMRI scans were assessed using the within-subject Wilcoxon signed-rank test in each disease group and in HC group ($\alpha = 0.05$). Owing to the small sample size, no correction for multiple comparisons was applied in either sMRI or dMRI analyses.

Standard Protocol Approvals, Registrations, and Patient Consents

Data were collected according to the NHS Research Ethics Committee protocols 16/SC/0224 and 17/EE/0246 for the Oxford cohort and according to the Southwest Veneto Territorial Ethic Committee (CET-ASOV) protocol 2413CESC for the Verona cohort. All patients provided written consent for inclusion of their anonymized data and MR images.

Data Availability

Anonymized data can be shared by request from any qualified investigator.

Results

Study Cohort

Twenty-two patients with MOGAD (Oxford n = 16, Verona n = 6), 33 patients with RRMS (Oxford n = 15, Verona n = 18), and 22 HCs (Oxford n = 13, Verona n = 9) were recruited.

We excluded 2 patients with MOGAD and 1 with RRMS because of relapses between the 2 study visits and a HC for having developed a concomitant CNS disease during the study. A total of 73 participants (20 with MOGAD, 32 with RRMS, and 21 HCs) were eventually included in the longitudinal clinical, brain MRI, and cognitive analyses (Figure 1). The median time from baseline assessment (T0) to follow-up (T1) was 16 months (range 12–56 months) in the MOGAD cohort, 17 months (range 12–42 months) in the RRMS cohort, and 17 months (range 12–45 months) in HCs ($p = 0.762$). The median time from T1 to confirmation EDSS visit was 11 months (range 6–46 months) in the MOGAD cohort and 14 months (range 6–59 months) in the RRMS group ($p = 0.170$).

No differences in age, sex at birth, and self-identified race group across the 3 groups and no differences in median EDSS scores and cognitive impairment prevalence between the 2 disease groups were found at T0 (Table 1). As per the inclusion and exclusion criteria, all patients did not change their maintenance therapy between the 2 assessments, although 70% of those with MOGAD and 21.9% of those with RRMS were not receiving disease-modifying therapy during the study period (Table 1).

Baseline Structural Brain MRI Data

At baseline sMRI, the RRMS cohort showed greater abnormalities than the MOGAD cohort in the median T2LN (22 in RRMS cohort [range 5–87] and 2 in MOGAD cohort [range 0–38], $p < 0.001$), cortical lesion number (1 in RRMS cohort [range 0–12] and 0 in MOGAD cohort [range 0–1], $p = 0.001$), and total lesion volume (3.33 cm^3 in RRMS cohort [range 0.47–34.2] and 0.23 cm^3 in MOGAD cohort [range 0–49.6], $p < 0.001$) (Table 1). Only 3 patients with MOGAD showed no brain lesions. The RRMS group showed lower normalized thalamic volume (5.74 ± 1.20 cm^3 in RRMS cohort and 6.52 ± 1.26 cm^3 in HCs, $p = 0.028$), normalized hippocampal volume (2.76 ± 0.58 cm^3 in RRMS cohort and 3.18 ± 0.65 cm^3 in HCs, $p = 0.018$), and normalized accumbens area (323.8 ± 99.9 mm^2 in RRMS cohort and 394.7 ± 94.1 mm^2 in HC, $p = 0.013$) compared with HCs while the MOGAD cohort showed a slight reduction in normalized GMV compared with HCs (726.22 ± 62.20 cm^3 in MOGAD cohort and 759.87 ± 38.24 cm^3 in HCs, $p = 0.042$). Although patients with RRMS showed greater baseline atrophy, the extent of atrophy did not differ between RRMS and MOGAD groups (eTable 3).

Baseline White Matter Microstructure Integrity

Overall, 627 white matter (WM) lesions were segmented. When lesions smaller than 40 mm^3 were excluded (n = 339, 54%), NODDI metrics were calculated for a total of 288 WM lesions (MOGAD cohort n = 38, RRMS cohort n = 250). Two of 14 patients with MOGAD did not present any lesions larger than 40 mm^3 while all 14 patients with RRMS had at least one WM lesion larger than 40 mm^3. At baseline dMRI analysis, ODI in nonlesional WM was greater in RRMS and MOGAD groups compared with HCs ($p = 0.006$). The RRMS group showed a reduced NDI ($p < 0.001$), an increase in the free water fraction ($p < 0.001$), and a diminished extraneurite water compartment ($p < 0.001$) in the WM lesions when contrasted with normal WM of HCs. The MOGAD group displayed a reduced NDI ($p < 0.001$) and a marginal elevation in ODI ($p = 0.045$) within WM lesions compared with normal WM of HCs. The mean ODI value was the only NODDI metric discriminating between MOGAD and RRMS WM lesions ($p = 0.007$) (eTable 3).

Table 1 Baseline Visit Demographic, Clinical, Cognitive, and Brain MRI Features of MOGAD, MS, and HC Cohorts

	MOGAD n = 20	RRMS n = 32	HC n = 21	MOGAD vs RRMS *p* value	MOGAD vs HC *p* value	RRMS vs HC *p* value
Clinical features						
Female, n (%)	11 (55)	15 (47)	11 (52)	0.776	0.867	0.782
Mean age ± SD	44.5 ± 13.1	41.4 ± 10.3	44 ± 13.3	0.336	0.904	0.415
Caucasian, n (%)	20 (100)	32 (100)	20 (95.2)	1.000	0.323	0.396
Mean age at onset ± SD	40 ± 11.7	33 ± 10.3	-	0.025	-	-
Median EDSS score (range)	2 (0–6.5)	2 (0–7)	-	0.854	-	-
Median disease duration, mo (range)	30 (6–252)	87.5 (6–294)	-	0.026	-	-
Median attacks before T0, n (range)	2 (1–7)	2 (1–6)	—	0.854	-	-
Median time from last attack to T0, mo (range)	13 (6–71)	42 (6–193)	—	0.003	-	-
Phenotypes at baseline (T0)						
Bilateral or monolateral ON, n (%)	12 (60)	10 (31.3)	-	0.040	-	-
Myelitis, n (%)	16 (80)	23 (71.9)	-	0.743	-	-
ADEM, n (%)	4 (20)	0 (0)	-	0.018	-	-
Cerebral monofocal or polyfocal deficits, n (%)	2 (10)	10 (31.3)	-	0.077	-	-
Cerebral cortical encephalitis ± seizures, n (%)	1 (5)	0 (0)	-	0.385	-	-
BS and cerebellar syndromes, n (%)	3 (15)	8 (25)	-	0.497	-	-
Cognitive features at baseline (T0)						
Education, mean y ± SD	13.8 ± 2.9	15.6 ± 4.1	-	0.104	-	-
Cognitive impairment prevalence, n (%) (20/30)[a]	4 (20)	8 (26.7)	-	0.740	-	-
Disease course						
Monophasic, n (%)	6 (30)	3 (9.4)	-	0.056	-	-
Relapsing, n (%)	14 (70)	29 (90.6)	-	0.056	-	-
Therapy during the study n (%)						
No treatments	14 (70)	7 (21.9)	-	<0.001	-	-
Oral steroids	4 (20)	0 (0)	-	0.019	-	-
Mycophenolate	2 (10)	0 (0)	-	0.149	-	-
Low-efficacy MS drugs[b]	0 (0)	15 (46.9)	-	<0.001	-	-
High-efficacy MS drugs[c]	0 (0)	10 (31.2)	-	0.004	-	-
Baseline MRI features						
Median time from last relapse, mo (range)	13 (6–71)	42 (6–193)	—	0.002	—	—
T2LN, median (range)	2 (0–38)	22 (5–87)	—	<0.001	—	—
T2LV, median (range), cm3	0.23(0–49.6)	3.33 (0.5–34.2)	—	<0.001	—	—
CLN, median (range)	0 (0–1)	1 (0–12)	-	0.001	-	-

Abbreviations: ADEM = acute disseminated encephalomyelitis; BS = brainstem; CLN = cortical lesion number; n = number; HC = healthy control; MOGAD = myelin oligodendrocyte glycoprotein antibody–associated disease; MS = multiple sclerosis; ON = optic neuritis; PASAT-3 = Paced Auditory Serial Addition Test-3 seconds; SDMT = Symbol Digit Modalities Test; T0 = baseline study time point; T2LN = T2-weighted image lesion number; T2LV = T2-weighted image lesion volume.

[a] Participants who underwent baseline cognitive assessment: MOGAD cohort n = 20; RRMS cohort n = 30.

[b] Dimethyl fumarate, interferon, teriflunomide, glatiramer acetate.

[c] Cladribine, natalizumab, anti-CD20$^+$ B-cell therapies.

Longitudinal Results

Clinical and Cognitive Progression Independent of Relapses

Clinical PIRA occurred in 2 of 32 patients with RRMS (6.25%) and in 0 of 20 patients with MOGAD (0%) (Fisher exact test $p = 0.762$, 1-β err prob = 0.38) in a median follow-up time of 17 months (range 12–45 months) and in a median follow-up time of 16 months (range 12–56 months), respectively (Kruskal-Wallis test $p = 0.400$) (Figure 2, A and B). The confirmation EDSS visit was performed at a median of 11 months (range 6–46 months) from T1 in the MOGAD group and at a median of 14 months (range 6–59 months) from T1 in the RRMS group ($p = 0.170$).

No patients with MOGAD showed brain T2LV reduction (lesion resolution) between the 2 MRI scans. New asymptomatic T2Ls were found in 8 of 32 patients with RRMS (25%) and 1 of 20 patients with MOGAD (5%) ($p = 0.065$). Only one of the 2 RRMS patients with PIRA also had new asymptomatic brain lesions.

The active MOGAD patient was diagnosed with clear positive MOGAD [onset longitudinally extensive transverse myelitis, high positive MOG-FL IgG titer (1:1,600), IgG1 positive, positive CSF oligoclonal bands] and presented 4 new asymptomatic T2Ls at T1 MRI compared with T0 MRI (two resembling MS lesions—small, periventricular, well-defined WM lesions), cognitive decline in verbal and visual memory learning and delayed recall tests, and stable low positive MOG-FL IgG titer (1:200; IgG1 positive). This patient presented with typical MOGAD at onset and then went on to develop typical MS. The following analyses were performed without the inclusion of this patient with MOG/MS overlap. The RRMS group showed a significant increase in median T2LV between the 2 MRI time points compared with the MOGAD group ($p = 0.014$).

Two patients with RRMS did not complete all the BRBNTs at 1 assessment and, therefore, were excluded from the cognitive analyses. Considering the remaining patients (RRMS n = 30; MOGAD n = 19), cognitive PIRA occurred in 2 of 30 patients with RRMS (6.67%) in a median cognitive follow-up of 17 months (range 12–42 months) and in 0 of 19 patients with MOGAD (0%) in a median cognitive follow-up of 16 months (range 12–56 months) (Figure 2C). One patient with MOGAD and the patient with MOG/MS overlap presented a cognitive decline preceding a relapse. The clinical and cognitive PIRA events occurred in the same 2 patients with RRMS: 1 patient with RRMS was off disease-modifying therapy, and the other was on ocrelizumab.

Longitudinal Analysis of Brain Volumetrics

Faster annual total DGMV loss (β = −0.510; 95% CI −0.920 to −0.099; $p = 0.015$), thalamic volume loss (β = −0.874; 95% CI −1.384 to −0.364; $p = 0.001$), and hippocampal volume loss (β = −1.269; 95% CI −2.230 to −0.308; $p = 0.010$) were observed in the RRMS group compared with the HC group (Table 2). By contrast, no differences in annual brain structure volume changes were found in the MOGAD group compared with HCs (Table 2). During the observation, greater annual thalamic atrophy (β = −0.742; 95% CI −1.310 to −0.171; $p = 0.011$) and annual hippocampus atrophy

Figure 2 Longitudinal Clinical and Cognitive Findings in MOGAD and RRMS Cohorts

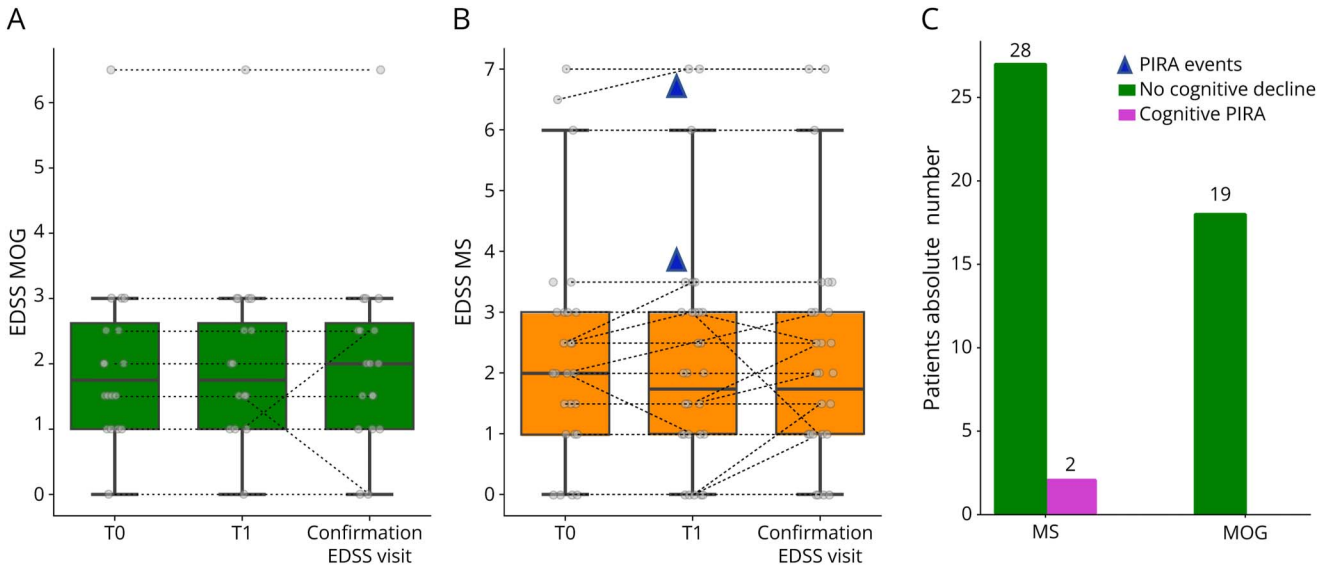

(A) EDSS evolution from T0 and T1 to last follow-up visit in the MOGAD cohort (no PIRA events). (B) EDSS evolution from T0 and T1 to last follow-up visit in RRMS (2 PIRA events confirmed). (C) Cognitive PIRA vs no cognitive decline and relapse-associated cognitive decline absolute number in patients with MOGAD and RRMS. The patient with MOG/MS overlap was excluded from this figure. EDSS = Expanded Disability Status Scale; Last-FU = last clinical follow-up; MOG = MOG antibody–associated disease; RRMS = relapsing-remitting MS; PIRA = progression independent of relapse activity; T0 = baseline visit; T1 = follow-up visit.

(β = −1.078; 95% CI −1.960 to −0.197; $p = 0.017$) were found in the RRMS group compared with patients with MOGAD (Table 2). Although reducing the power of the analysis (power 1-β form 0.44 to 0.38, effect size 0.15, $\alpha = 0.05$), these results were confirmed either by excluding the 4 patients with MOGAD on low-dose oral steroid therapy during the study period (annual thalamic atrophy β = −0.707; 95% CI −1.330 to −0.083; $p = 0.026$, and annual hippocampal atrophy β = −0.992; 95% CI −1.942 to −0.042; $p = 0.041$) or by excluding the 3 patients with MOGAD without brain lesions at baseline (annual thalamic atrophy β = −0.802; 95% CI −1.403 to −0.202; $p = 0.009$, and annual hippocampal atrophy β = −1.029; 95% CI −1.964 to −0.093; $p = 0.031$) (power 1-β = 0.40, effect size 0.15, $\alpha = 0.05$). In addition, in the MOGAD cohort, neither the steroid uptake nor the presence of brain lesions at the T0 MRI was significantly associated with annualized thalamic and hippocampal volume change.

Figure 3 illustrates examples of mean annualized thalamic and hippocampal volume changes in patients with RRMS, patients with MOGAD, and HC participants.

Longitudinal White Matter Microstructure Integrity Change

Overall, 304 WM lesions were longitudinally monitored on dMRI. Among these, 16 new asymptomatic WM lesions larger than 40 mm^3 were identified in the RRMS group and none in the MOGAD group. NODDI map analyses did not reveal any difference in longitudinal variation of neurite density, free water fraction, and extraneurite indices in nonlesional WM of the disease groups and in normal WM of HCs. The RRMS group showed a significant increase in longitudinal free water fraction in lesional WM ($p = 0.016$) (Table 3) even when new asymptomatic WM lesions were excluded from the analyses ($p = 0.008$). MOGAD did not show any longitudinal changes in chronic WM lesions

Table 2 Mixed-Effect Regression Assessing the Effect of the MOGAD and RRMS Groups on the Longitudinal Brain MRI Volumetrics

	MOGAD (ref) vs RRMS		MOGAD vs HC (ref)		RRMS vs HC (ref)	
	β coefficient	95% CI *p* value	β coefficient	95% CI *p* value	β coefficient	95% CI *p* value
Annualized PBVC	−0.213	−0.608 to 0.182 0.291	0.085	−0.278 to 0.449 0.646	−0.038	−0.4045 to 0.329 0.840
Annualized TBV pc	−0.022	−0.415 to 0.369 0.910	0.126	−0.297 to 0.549 0.560	−0.277	−0.646 to 0.090 0.139
Annualized cortex vol pc	0.051	−0.590 to 0.005 0.877	0.453	−0.209 to 1.116 0.180	−0.064	−0.732 to 0.603 0.849
Annualized DGMV pc	−0.443	−0.891 to 0.315 0.053	−0.010	−0.5240 to 0.504 0.969	−0.510	−0.920 to −0.099 **0.015**
Annualized WMV pc	−0.134	−0.670 to 0.401 0.623	0.009	−0.5070 to 0.526 0.971	−0.398	−1.088 to 0.291 0.257
Annualized CTh pc	0.144	−0.398 to 0.697 0.603	0.394	−0.228 to 1.017 0.214	−0.008	−0.662 to 0.645 0.979
Annualized thalamic vol pc	−0.742	−1.310 to −0.171 **0.011**	−0.111	−0.807 to 0.584 0.754	−0.874	−1.384 to −0.364 **0.001**
Annualized caudate vol pc	−1.11	−2.361 to 0.146 0.083	−0.137	−1.459 to 1.184 0.839	−1.093	−2.268 to 0.081 0.068
Annualized putamen vol pc	−0.067	−0.834 to 0.701 0.864	−0.412	−1.095 to 0.270 0.236	−0.885	−1.801- to 0.031 0.058
Annualized pallidum vol pc	0.558	−0.593 to 1.709 0.342	0.132	−1.315 to 1.579 0.858	0.408	−0.793 to 1.610 0.505
Annualized hippocampus vol pc	−1.078	−1.960 to −0.197 **0.017**	0.747	−0.757 to 2.251 0.330	−1.269	−2.230 to −0.308 **0.010**
Annualized amygdala vol pc	−0.620	−1.700 to 0.459 0.260	−0.630	−2.122 to 0.861 0.407	−0.214	−1.627 to 1.198 0.766
Annualized accumbens area pc	−4.039	−8.427 to 0.348 0.071	−0.187	−6.009 to 5.634 0.950	−0.214	−1.627 to 1.198 0.766

Abbreviations: CTh = mean cortical thickness; DGMV = deep gray matter volume; PBVC = percentage of brain volume change calculated with SIENA FSL package; pc = percentage change with respect to time point T0 using FreeSurfer longitudinal stream; ref = reference category; TBV = total brain volume; vol = volume; WMV = white matter volume.
Mixed-effect models with longitudinal brain MRI volumetrics as the dependent variable; disease category as the explanatory variable; age, sex, time from last relapse, and new T2Ls as explanatory covariates; and MRI protocol (center) as the random intercept.
Bolded entries are signficant *p*-values < 0.05.

Figure 3 Baseline and Follow-Up 3D T1-Weighted MRI Showing Annualized Thalamic and Hippocampal Volume Percentage Changes in RRMS and MOGAD Groups and Controls

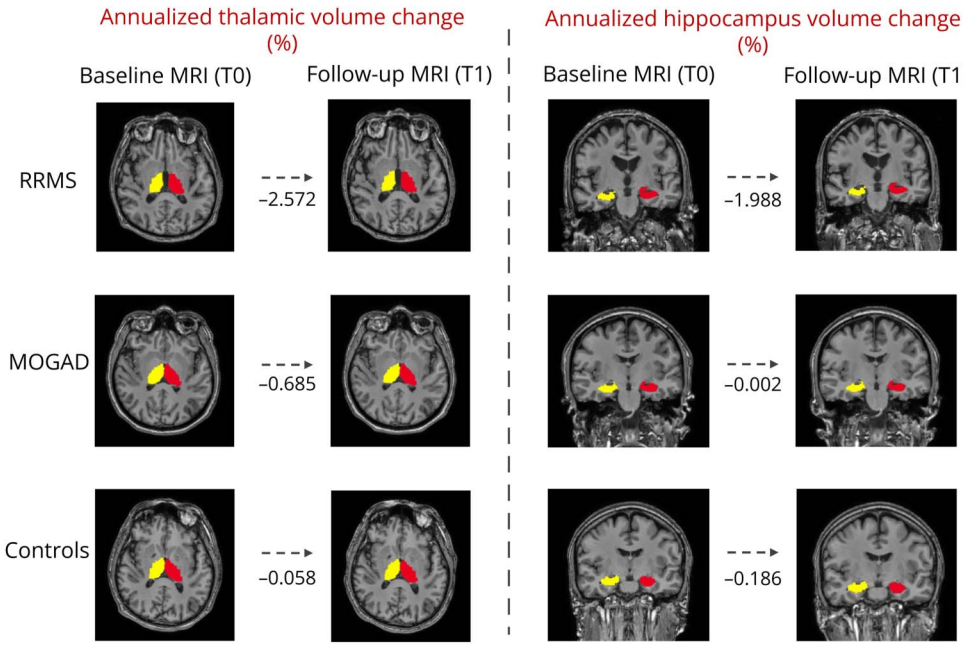

Three examples for each group of participants (RRMS, MOGAD, and controls) illustrate the key differences in brain volumetrics found using mixed-effects models: on the left, annualized mean thalamic volume change; on the right, annualized mean hippocampal volume change, both lower in the RRMS cohort compared with MOGAD and HC cohorts. HCs = healthy controls; MOGAD = MOG antibody–associated disease; RRMS = relapsing-remitting MS.

regardless of new asymptomatic lesions considered (Table 3, Figure 4).

Discussion

In this study, we integrated prospective assessments of EDSS, cognitive function, brain volumetrics, and microstructural diffusion neuroimaging to investigate evidence of PIRA and subclinical neurodegenerative processes in both clinically stable MOGAD and RRMS groups in comparison with a group of HCs. In summary, we found the following: (1) at baseline analysis, the RRMS group exhibited greater lesional white matter microstructural damage compared with the MOGAD group; (2) at longitudinal analysis, a proportion of patients with RRMS experienced clinical (6.25%) and cognitive (6.67%) PIRA while no individuals with MOGAD experienced PIRA; (3) the RRMS group exhibited a faster subclinical volumetric loss of DGM structures and displayed a significant progressive increase in free water content in WM lesions compared with HCs; by contrast, the MOGAD group did not present brain volumetric changes over time and showed no microstructural longitudinal dMRI differences within either lesional or NLWM compared with HCs; and of interest, (4) the RRMS group showed a higher rate of thalamic and hippocampal volume loss compared with the MOGAD group.

Baseline Clinical and Imaging Features of Neurodegeneration

Patients with MS had a higher baseline load of white and gray matter lesions and more extensive microstructural damage identified using NODDI metrics compared with patients with MOGAD. Specifically, RRMS dMRI analysis showed reduced lesional neurite density, increased lesional free water, and reduced lesional neurite orientation dispersion compared with the NWM of HCs. By contrast, the MOGAD group showed reduced lesional WM neurite density and a slight increase in neurite orientation dispersion relative to normal WM. In addition, the RRMS group had significantly lower baseline lesional neurite orientation dispersion compared with the MOGAD group.

These differences in dMRI features may reflect the distinct and milder patterns of MOGAD lesional damage compared with RRMS, as described in pathologic studies. MOGAD lesions are characterized by myelin loss, axonal spheroids, and relatively preserved oligodendrocytes and axons while MS lesions involve myelin and mature oligodendrocyte loss, variable axonal degeneration, and activated microglia.

In addition, both MOGAD and RRMS groups had higher orientation dispersion in NLWM than HCs. Because approximately half of our MOGAD cohort experienced brain attacks before recruitment, we suggest that NLWM damage in MOGAD might result from incomplete microstructural recovery after previous acute brain lesions.

Longitudinal Clinical and Imaging Features of Neurodegeneration

The absence of significant longitudinal changes in all brain volumetrics assessed in the MOGAD group compared with HCs suggests a lack of significant subclinical brain neurodegenerative

Table 3 NODDI Map Longitudinal Paired *t* Test Analyses in MOGAD, RRMS, and HC Cohorts

	MOGAD, N = 14			RRMS, N = 14			HC, N = 12		
	T0	T1	*p* Value [a]	T0	T1	*p* Value	T0	T1	*p* Value [a]
NAWM									
NDI	0.551 ± 0.017	0.552 ± 0.016	0.259	0.543 ± 0.027	0.543 ± 0.029	0.683	0.510 ± 0.154	0.521 ± 0.028	0.389
ISOVF	0.058 ± 0.009	0.060 ± 0.009	0.065	0.063 ± 0.007	0.065 ± 0.011	0.165	0.059 ± 0.020	0.062 ± 0.008	0.337
ODI	0.255 ± 0.018	0.254 ± 0.017	0.644	0.256 ± 0.017	0.257 ± 0.018	0.430	0.221 ± 0.067	0.247 ± 0.023	0.198
New and chronic WM T2L									
NDI	0.312 ± 0.067	0.310 ± 0.077	0.630	0.312 ± 0.048	0.310 ± 0.045	0.217	—	—	—
ISOVF	0.100 ± 0.082	0.109 ± 0.088	0.522	0.124 ± 0.039	0.132 ± 0.040	**0.016**	—	—	—
ODI	0.238 ± 0.092	0.231 ± 0.099	0.084	0.167 ± 0.027	0.165 ± 0.028	0.149	—	—	—
Chronic WM T2L									
NDI	0.312 ± 0.067	0.290 ± 0.100	0.205	0.312 ± 0.048	0.309 ± 0.046	0.341	—	—	—
ISOVF	0.100 ± 0.082	0.115 ± 0.151	0.194	0.124 ± 0.039	0.132 ± 0.039	**0.008**	—	—	—
ODI	0.238 ± 0.092	0.249 ± 0.094	0.331	0.167 ± 0.027	0.166 ± 0.027	0.438	—	—	—

Abbreviations: HC = healthy control; ISOVF = isotropic volume fraction; MOGAD = myelin oligodendrocyte glycoprotein antibody–associated disease; NAWM = normal-appearing white matter; NDI = neurite density index; ODI = orientation dispersion; RRMS = relapsing-remitting multiple sclerosis; T2L = T2/FLAIR hyperintense lesions; WM = white matter.
The bold p-values corrispond to $p < 0.05$.

Figure 4 Longitudinal Diffusion MRI Findings in MOGAD, RRMS, and HC Cohorts

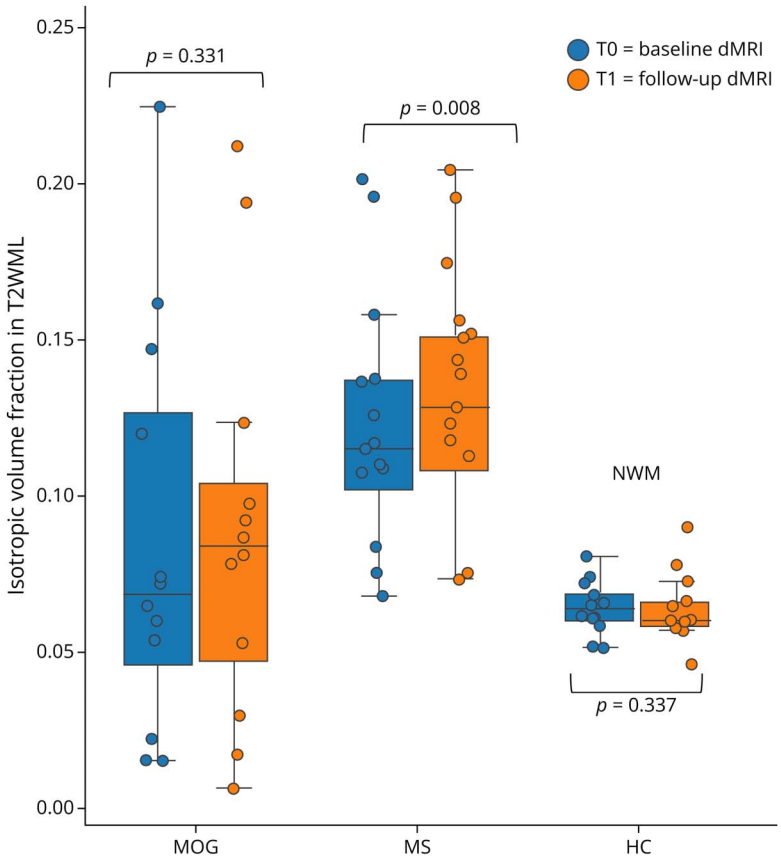

Longitudinal evolution of isotropic volume fraction in MOGAD and RRMS T2 weighted hyperintense white matter lesions (T2WML) vs normal white matter tissue in HC. The patient with MOG/MS overlap was excluded. dMRI = diffusion-weigheted imaging; HC = healthy control; MOG = MOG antibody–associated disease; RRMS = relapsing-remitting multiple sclerosis; NWM = normal white matter; T0 = baseline; T1 = follow-up; T2WML = T2/FLAIR hyperintense white matter lesion.

processes independent of inflammatory attacks in MOGAD within the examined timespan. This contrasts with the significantly faster reduction of DGM volumetrics observed in the RRMS group compared with HCs. The thalamus and hippocampus were identified as the most sensitive structures for differentiating RRMS from MOGAD. DGM structures and hippocampi, which are affected early in the MS disease course and exhibit faster annual atrophy rates compared with other GM brain structures,[34-36] allowed us to detect neurodegenerative processes in RRMS despite the relatively short follow-up. A small retrospective MRI analysis revealed greater DGM atrophy in MOGAD compared with MS,[20] but it did not account for clinical stability periods, age, sex, or timing from the last attack. These findings may reflect a greater impact of inflammatory attacks on gray matter in MOGAD than in MS, rather than relapse-independent neurodegenerative processes.[26]

Our study used NODDI maps to analyze WM tissue integrity changes over time in the MOGAD group. Only the RRMS group showed a significant increase in lesional free water compared with baseline dMRI, even when excluding new asymptomatic lesions. These changes were not observed in MOGAD lesions or nonlesional WM of both RRMS and MOGAD groups, supporting the presence of chronic active microstructural changes in RRMS lesions but not in MOGAD. Notably, this finding is consistent with previous studies documenting increased free water fraction in MS lesions.[37]

During follow-up, clinical and cognitive PIRA was observed exclusively in the RRMS group, although the difference with MOGAD was not significant. This may be due to the inclusion of stable RRMS patients during remission, short follow-up, and low statistical power. Larger sample sizes or longer follow-up would likely make the differences significant, as supported by other reports.[9,18,19,38] This demonstrates the value of imaging surrogates in detecting subclinical neurodegeneration, which differed significantly between the 2 disease groups.

We investigated cognitive decline independent of relapse activity (cognitive PIRA) in a MOGAD cohort compared with an RRMS cohort using a well-validated battery of neuropsychological tests (BRBNTs) assessing a wide range of cognitive domains. Although a recent definition of cognitive PIRA has been proposed in MS,[4] our study used Rao's BRB, which offers a broader evaluation of cognitive function because no validated cognitive batteries are available in MOGAD. We adopted a criterion of a reduction in z-scores by at least one SD in at least two BRB subtests outside relapses. Despite matched baseline cognitive scores, people with MOGAD did not have cognitive PIRA in line with a recent published paper,[39] whereas this was observed in the RRMS group, including those with EDSS worsening not related to change in the cognitive function section of the Kurtzke score.

This study has several limitations. First, the small cohort size and the short, irregular MRI and cognitive follow-up duration pose challenges in capturing more subtle neurodegenerative changes. The small sample size and the explorative nature of the study could reduce the generalizability of our findings to larger populations, although in clinical practice, we have not observed progression in our patients with MOGAD, unlike in patients with MS. Therefore, longer follow-up outside relapses would be particularly useful in MOGAD and in separate cohorts. In addition, most individuals with RRMS were treated with disease-modifying therapy, whereas most patients with MOGAD were not. The differential treatment status could potentially underestimate differences between the 2 diseases although it supports the clinical literature of PIRA in MS[1] and not MOGAD.[22] The use of BRBNTs may create comparability issues with previous MS studies that used Brief International Cognitive Assessment fo multiple sclerosis (BICAMS) for assessing cognitive PIRA because of different neuropsychological test batteries. However, with no current guidelines for cognitive assessment in patients with MOGAD, a comprehensive battery like BRB is warranted. The dMRI results must be interpreted cautiously because they were derived from a small cohort of patients, and their pathologic specificity needs validation in larger and different disease cohorts.[37] Finally, the lack of adjustment for multiple comparisons might increase the risk of type *I* errors.

In this prospective clinical, cognitive, and advanced imaging study, patients with MOGAD did not show significant clinical or subclinical neurodegeneration independent of inflammatory attacks compared with patients with MS. Thalamic and hippocampal volumetrics and lesional NODDI metrics were useful in differentiating MOGAD from MS. If validated, these observations may influence clinical management and trial design for MOGAD, emphasizing the monitoring of inflammatory attacks rather than neurodegenerative progression. This contrasts with MS, where PIRA is recognized as a major determinant of disability accumulation.[40] Further longer follow-up studies in different cohorts, with identical imaging intervals, are needed to confirm our findings and rule out subtle neurodegenerative changes in MOGAD, although our findings support our clinical and experts' opinion that the clinical course of MOGAD is monophasic or relapsing but not progressive.[22]

Acknowledgment

The authors thank MS society innovative grant (B006-18.1) for supporting this study, the highly specialized commissioning team for funding the Neuromyelitis Optica service in Oxford, and all the staff at the Wellcome Centre for Integrative Neuroimaging (WIN). The authors also thank the MRI radiographers of the Verona University Hospital who helped with the MRI acquisitions, Mr James Moore, and Dr. Angela Peloso for contributing to the study organization and MRI sequences armonizations between centers. The authors also thank the participants and their relatives, in Oxford and Verona.

Author Contributions

V. Camera: drafting/revision of the manuscript for content, including medical writing for content; major role in the

acquisition of data; study concept or design; analysis or interpretation of data. S. Messina: drafting/revision of the manuscript for content, including medical writing for content; major role in the acquisition of data; study concept or design; analysis or interpretation of data. A. Tamanti: major role in the acquisition of data; study concept or design; analysis or interpretation of data. P. Bontempi: study concept or design; analysis or interpretation of data. L.S. Petralia: analysis or interpretation of data. L. Griffanti: study concept or design; analysis or interpretation of data. M. Pitteri: analysis or interpretation of data. M. Guandalini: major role in the acquisition of data. F.B. Pizzini: major role in the acquisition of data. G.C. DeLuca: drafting/revision of the manuscript for content, including medical writing for content; analysis or interpretation of data. M.I.S. Leite: drafting/revision of the manuscript for content, including medical writing for content; study concept or design. A. Daducci: major role in the acquisition of data; analysis or interpretation of data. R. Geraldes: drafting/revision of the manuscript for content, including medical writing for content; analysis or interpretation of data. M. Calabrese: drafting/revision of the manuscript for content, including medical writing for content; major role in the acquisition of data. J. Palace: drafting/revision of the manuscript for content, including medical writing for content; major role in the acquisition of data; study concept or design; analysis or interpretation of data.

Study Funding

The study was partly funded by Roche Pharma. The authors thank the highly specialized commissioning team for funding the Neuromyelitis Optica Service in Oxford. MRI scans were funded by a Research and Development fund and a Multiple Sclerosis Society Innovative grant (B006–18.1) belonging to the principal investigator. J.A. Palace and L. Griffanti are supported by an Alzheimer's Association grant (AARF-21-846366) and by the National Institute for Health Research (NIHR) Oxford Health Biomedical Research Centre (BRC) (NIHR203316). This work was also partly supported by the Wellcome Centre for Integrative Neuroimaging, which has core funding from the Wellcome Trust (203139/Z/16/Z and 203139/A/16/Z). For the purpose of open access, the author has applied a CC-BY public copyright licence to any Author Accepted.

Disclosure

This study was partially sponsored by Roche. V. Camera received European Charcot Foundation fellowship grant, honoraria for speaking, and travel grants for scientific meetings from Roche, Jansen, BMS, Novartis, Alexion, and Amgen; received honoraria for advisory work from Novartis; and is a Member of the European Charcot Foundation young investigators/fellow. S. Messina received speaking honoraria from UCB and travel grants from Sanofi, UCB, Merck, Alexion, and Roche. A. Tamanti, P. Bontempi, and L.S. Petralia report no disclosures. L. Griffanti received royalties from licensing of FSL to nonacademic, commercial parties. M. Pitteri, M. Guandalini, and F.B. Pizzini report no disclosures. G.C. DeLuca has received support from the NIHR Biomedical Research Centre (BRC), Oxford; and received research funding from Oxford BRC, MRC (United Kingdom), the UK MS Society, National Health and Medical Research (Australia), the Department of Defense (USA), the European Charcot Foundation, the American Academy of Neurology (AAN), Merck-Serono, and Oxford-Quinnipiac Partnership; has received travel expenses from Genzyme, Merck Serono, Novartis, Roche, the MS Academy, and the AAN; and has received honoraria as an invited speaker or faculty for Novartis, Roche, the MS Academy, and the AAN. A. Daducci reports no disclosures. M.I.S. Leite is funded by the NHS (Myasthenia and Related Disorders Service and National Specialized Commissioning Group for Neuromyelitis Optica, United Kingdom) and by the University of Oxford, United Kingdom; has been awarded research grants from the UK Association for Patients with Myasthenia (Myaware), Muscular Dystrophy Campaign (MDUK), and the University of Oxford; has received speaker honoraria and travel grants from UCB Pharma and Horizon Therapeutics; has received consultancy fees from UCB Pharma; and serves on scientific or educational advisory boards for UCB Pharma, Argenx, and Horizon Therapeutics, and on the steering committee for Horizon Therapeutics. R. Geraldes has received support for scientific meetings and courses from Bayer, Biogen, Merck, Novartis, and Janssen; and has received honoraria for advisory work or talks from Biogen, Novartis, UCB, and MIAC. M. Calabrese received honoraria for research or speaking and travel grants from Roche, Biogen Idec, Sanofi-Genzyme, Novartis, and BMS; received grant research from Italian Health Minister; and received honoraria for advisory work from Novartis, Roche, Merck, and BMS, Biogen. J. Palace has received support for scientific meetings and honoraria for advisory work from Merck Serono, Novartis, Chugai, Alexion, Roche, Medimmune, Amgen, Vitaccess, UCB, Mitsubishi, Amplo, and Janssen; has received grants from Alexion, Argenx, Clene, Roche, Medimmune, and Amplo Biotechnology; holds Patent ref P37347WO and licence agreement Numares multimarker MS diagnostics Shares in AstraZenica; her group has been awarded an ECTRIMS fellowship and a Sumaira Foundation grant to start later this year; a Charcot fellow worked in Oxford 2019–2021; she acknowledges partial funding to the trust by highly specialised services NHS England; is on the medical advisory boards of the Sumaira Foundation and MOG project charities; is a member of the Guthy Jackon Foundation Charity; is on the board of the European Charcot Foundation; is a member of MAGNIMS and the UK NHSE IVIG Committee; is chairperson of the NHSE neuroimmunology patient pathway; has been an ECTRIMS council member on the educational committee since June 2023; is currently on the ABN advisory groups for MS and neuroinflammation; and was recently on a neuromuscular diseases advisory group. Go to Neurology.org/OA for full disclosures.

Publication History

Received by *Neurology® Open Access* November 4, 2024. Accepted in final form March 11, 2025. Submitted and externally peer reviewed. The handling editor was Amy Kunchok, MBBS, MMed, FRACP, PhD.

References

1. Kappos L, Wolinsky JS, Giovannoni G, et al. Contribution of relapse-independent progression vs relapse-associated worsening to overall confirmed disability accumulation in typical relapsing multiple sclerosis in a pooled analysis of 2 randomized clinical trials. *JAMA Neurol*. 2020;77(9):1132-1140. doi:10.1001/jamaneurol.2020.1568
2. Ciccarelli O, Barkhof F, Calabrese M, et al. Using the progression independent of relapse activity framework to unveil the pathobiological foundations of multiple sclerosis. *Neurology*. 2024;103(1):e209444. doi:10.1212/WNL.0000000000209444
3. Calabrese M, Preziosa P, Scalfari A, et al. Determinants and biomarkers of progression independent of relapses in multiple sclerosis. *Ann Neurol*. 2024;96(1):1-20. doi:10.1002/ana.26913
4. Fuchs TA, Schoonheim MM, Zivadinov R, et al. Cognitive progression independent of relapse in multiple sclerosis. *Mult Scler*. 2024;30(11-12):1468-1478. doi:10.1177/13524585241256540
5. Eijlers AJC, van Geest Q, Dekker I, et al. Predicting cognitive decline in multiple sclerosis: a 5-year follow-up study. *Brain*. 2018;141(9):2605-2618. doi:10.1093/brain/awy202
6. Aarsland D, Creese B, Politis M, et al. Cognitive decline in Parkinson disease. *Nat Rev Neurol*. 2017;13(4):217-231. doi:10.1038/nrneurol.2017.27
7. Rabin LA, Smart CM, Amariglio RE. Subjective cognitive decline in preclinical Alzheimer's disease. *Annu Rev Clin Psychol*. 2017;13:369-396. doi:10.1146/annurev-clinpsy-032816-045136
8. Filippi M, Preziosa P, Barkhof F, et al. Diagnosis of progressive multiple sclerosis from the imaging perspective: a review. *JAMA Neurol*. 2021;78(3):351-364. doi:10.1001/jamaneurol.2020.4689
9. Cagol A, Schaedelin S, Barakovic M, et al. Association of brain atrophy with disease progression independent of relapse activity in patients with relapsing multiple sclerosis. *JAMA Neurol*. 2022;79(7):682-692. doi:10.1001/jamaneurol.2022.1025
10. Coupé P, Planche V, Mansencal B, et al. Lifespan neurodegeneration of the human brain in multiple sclerosis. *Hum Brain Mapp*. 2023;44(17):5602-5611. doi:10.1002/hbm.26464
11. Ghione E, Bergsland N, Dwyer MG, et al. Brain atrophy is associated with disability progression in patients with MS followed in a clinical routine. *AJNR Am J Neuroradiol*. 2018;39(12):2237-2242. doi:10.3174/ajnr.A5876
12. Klaver R, Popescu V, Voorn P, et al. Neuronal and axonal loss in normal-appearing gray matter and subpial lesions in multiple sclerosis. *J Neuropathol Exp Neurol*. 2015;74(5):453-458. doi:10.1097/NEN.0000000000000189
13. Popescu V, Klaver R, Voorn P, et al. What drives MRI-measured cortical atrophy in multiple sclerosis? *Mult Scler*. 2015;21(10):1280-1290. doi:10.1177/1352458514562440
14. Rocca MA, Battaglini M, Benedict RHB, et al. Brain MRI atrophy quantification in MS: from methods to clinical application. *Neurology*. 2017;88(4):403-413. doi:10.1212/WNL.0000000000003542
15. Seyedmirzaei H, Nabizadeh F, Aarabi MH, Pini L. Neurite orientation dispersion and density imaging in multiple sclerosis: a systematic review. *J Magn Reson Imaging*. 2023;58(4):1011-1029. doi:10.1002/jmri.28727
16. Grussu F, Schneider T, Tur C, et al. Neurite dispersion: a new marker of multiple sclerosis spinal cord pathology? *Ann Clin Transl Neurol*. 2017;4(9):663-679. doi:10.1002/acn3.445
17. Lakhani DA, Schilling KG, Xu J, Bagnato F. Advanced multicompartment diffusion MRI models and their application in multiple sclerosis. *AJNR Am J Neuroradiol*. 2020;41(5):751-757. doi:10.3174/ajnr.A6484
18. Molazadeh N, Akaishi T, Bose G, Nishiyama S, Chitnis T, Levy M. Progression independent of relapses in aquaporin4-IgG-seropositive neuromyelitis optica spectrum disorder, myelin oligodendrocyte glycoprotein antibody-associated disease, and multiple sclerosis. *Mult Scler Relat Disord*. 2023;80:105093. doi:10.1016/j.msard.2023.105093
19. Akaishi T, Misu T, Takahashi T, et al. Progression pattern of neurological disability with respect to clinical attacks in anti-MOG antibody-associated disorders. *J Neuroimmunol*. 2021;351:577467. doi:10.1016/j.jneuroim.2020.577467
20. Lotan I, Billiet T, Ribbens A, et al. Volumetric brain changes in MOGAD: a cross-sectional and longitudinal comparative analysis. *Mult Scler Relat Disord*. 2023;69:104436. doi:10.1016/j.msard.2022.104436
21. Amin M, Al-iedani O, Lea RA, Brilot F, Maltby VE, Lechner-Scott J. A longitudinal analysis of brain volume changes in myelin oligodendrocyte glycoprotein antibody-associated disease. *J Neuroimaging*. 2024;34(1):78-85. doi:10.1111/jon.13175
22. Banwell B, Bennett JL, Marignier R, et al. Diagnosis of myelin oligodendrocyte glycoprotein antibody-associated disease: international MOGAD Panel proposed criteria. *Lancet Neurol*. 2023;22(3):268-282. doi:10.1016/S1474-4422(22)00431-8
23. Thompson AJ, Banwell BL, Barkhof F, et al. Diagnosis of multiple sclerosis: 2017 revisions of the McDonald criteria. *Lancet Neurol*. 2018;17(2):162-173. doi:10.1016/S1474-4422(17)30470-2
24. Mariano R, Messina S, Roca-Fernandez A, Leite MI, Kong Y, Palace JA. Quantitative spinal cord MRI in MOG-antibody disease, neuromyelitis optica and multiple sclerosis. *Brain*. 2021;144(1):198-212. doi:10.1093/brain/awaa347
25. Cortese R, Battaglini M, Prados F, et al. Clinical and MRI measures to identify non-acute MOG-antibody disease in adults. *Brain*. 2023;146(6):2489-2501. doi:10.1093/brain/awac480
26. Messina S, Mariano R, Roca-Fernandez A, et al. Contrasting the brain imaging features of MOG-antibody disease, with AQP4-antibody NMOSD and multiple sclerosis. *Mult Scler*. 2022;28(2):217-227. doi:10.1177/13524585211018987
27. Cacciaguerra L, Redenbaugh V, Chen JJ, et al. Timing and predictors of T2-lesion resolution in patients with myelin oligodendrocyte glycoprotein antibody-associated disease. *Neurology*. 2023;101(13):e1376-e1381. doi:10.1212/WNL.0000000000207478
28. Camp SJ, Stevenson VL, Thompson AJ, et al. Cognitive function in primary progressive and transitional progressive multiple sclerosis: a controlled study with MRI correlates. *Brain*. 1999;122 (Pt 7)(Pt 7):1341-1348. doi:10.1093/brain/122.7.1341
29. Amato MP, Portaccio E, Goretti B, et al. The Rao's Brief Repeatable Battery and Stroop Test: normative values with age, education and gender corrections in an Italian population. *Mult Scler*. 2006;12(6):787-793. doi:10.1177/1352458506070933
30. Amato MP, Portaccio E, Goretti B, et al. Relevance of cognitive deterioration in early relapsing-remitting MS: a 3-year follow-up study. *Mult Scler*. 2010;16(12):1474-1482. doi:10.1177/1352458510380089
31. Jenkinson M, Beckmann CF, Behrens TEJ, Woolrich MW, Smith SM. FSL. *Neuroimage*. 2012;62(2):782-790. doi:10.1016/j.neuroimage.2011.09.015
32. Smith SM, Zhang Y, Jenkinson M, et al. Accurate, robust, and automated longitudinal and cross-sectional brain change analysis. *Neuroimage*. 2002;17(1):479-489. doi:10.1006/nimg.2002.1040
33. Reuter M, Schmansky NJ, Rosas HD, Fischl B. Within-subject template estimation for unbiased longitudinal image analysis. *Neuroimage*. 2012;61(4):1402-1418. doi:10.1016/j.neuroimage.2012.02.084
34. Eshaghi A, Prados F, Brownlee WJ, et al. Deep gray matter volume loss drives disability worsening in multiple sclerosis. *Ann Neurol*. 2018;83(2):210-222. doi:10.1002/ana.25145
35. Bishop CA, Newbould RD, Lee JS, et al. Analysis of ageing-associated grey matter volume in patients with multiple sclerosis shows excess atrophy in subcortical regions. *Neuroimage Clin*. 2017;13:9-15. doi:10.1016/j.nicl.2016.11.005
36. Papadopoulos D, Dukes S, Patel R, Nicholas R, Vora A, Reynolds R. Substantial archaeocortical atrophy and neuronal loss in multiple sclerosis. *Brain Pathol*. 2009;19(2):238-253. doi:10.1111/j.1750-3639.2008.00177.x
37. York EN, Meijboom R, Thrippleton MJ, et al. Longitudinal microstructural MRI markers of demyelination and neurodegeneration in early relapsing-remitting multiple sclerosis: magnetisation transfer, water diffusion and g-ratio. *Neuroimage Clin*. 2022;36:103228. doi:10.1016/j.nicl.2022.103228
38. Gärtner J, Hauser SL, Bar-Or A, et al. Efficacy and safety of ofatumumab in recently diagnosed, treatment-naive patients with multiple sclerosis: results from ASCLEPIOS I and II. *Mult Scler*. 2022;28(10):1562-1575. doi:10.1177/13524585221078825
39. Passoke S, Stern C, Häußler V, et al. Cognition in patients with myelin oligodendrocyte glycoprotein antibody-associated disease: a prospective, longitudinal, multicentre study of 113 patients (CogniMOG-Study). *J Neurol Neurosurg Psychiatry*. 2024;96(3):296-305. doi:10.1136/jnnp-2024-333994
40. Portaccio E, Betti M, De Meo E, et al. Progression independent of relapse activity in relapsing multiple sclerosis: impact and relationship with secondary progression. *J Neurol*. 2024;271(8):5074-5082. doi:10.1007/s00415-024-12448-4